

# Optimal qudit overlapping tomography and optimal measurement order

Shuowei Ma,<sup>1</sup> Qianfan Wang,<sup>2</sup> Lvzhou Li,<sup>1</sup> and Fei Shi<sup>1,\*</sup>

<sup>1</sup>*School of Computer Science and Engineering, Sun Yat-sen University, Guangzhou 510006, China*  
<sup>2</sup>*Department of Computer Science, City University of Hong Kong, Hong Kong SAR, China*

Quantum state tomography is essential for characterizing quantum systems, but it becomes infeasible for large systems due to exponential resource scaling. Overlapping tomography addresses this challenge by reconstructing all  $k$ -body marginals using few measurement settings, enabling the efficient extraction of key information for many quantum tasks. While optimal schemes are known for qubits, the extension to higher-dimensional qudit systems remains largely unexplored. Here, we investigate optimal qudit overlapping tomography, constructing local measurement settings from generalized Gell-Mann matrices. By establishing a correspondence with combinatorial covering arrays, we present two explicit constructions of optimal measurement schemes. For  $n$ -qutrit systems, we prove that pairwise tomography requires at most  $8 + 56 \lceil \log_8 n \rceil$  measurement settings, and provide an explicit scheme achieving this bound. Furthermore, we develop an efficient algorithm to determine the optimal order of these measurement settings, minimizing the experimental overhead associated with switching configurations. Compared to the worst-case ordering, our optimized schedule reduces switching costs by approximately 50%. These results provide a practical pathway for efficient characterization of qudit systems, facilitating their application in quantum communication and computation.

## I. INTRODUCTION

Quantum state tomography (QST) is a fundamental tool in quantum information science, enabling the reconstruction of unknown quantum states through a series of measurements [1–3]. However, traditional QST becomes prohibitively resource-intensive as the system size increases, requiring an exponential number of measurements to fully characterize the state. In contrast, many quantum information tasks require only information about marginal states rather than the full quantum state [4–8]. Overlapping tomography focuses on reconstructing all  $k$ -body marginals using a small number of local measurement settings [9]. This approach is particularly useful for measuring many-body entanglement and correlation functions [10], diagnosing long-range order and critical behavior, characterizing topological order [11–13], and estimating expectation values of  $k$ -local Hamiltonians [14–17].

Optimal qubit overlapping tomography seeks to determine the minimum number of Pauli measurement settings required to reconstruct all  $k$ -body marginals [13, 18–21]. This problem is closely connected to the covering number of covering arrays [19]—a combinatorial structure widely used in experimental design and testing [22–25]. While most research on optimal overlapping tomography has focused on qubit systems, optimal qudit overlapping tomography remains largely unexplored. Qudit systems, which generalize qubits to  $d$ -level quantum systems, support more complex protocols and can significantly enhance the security and capacity of quantum communication [26–30]. Efficient tomography is essential for harnessing these advantages in practical applications.

Additionally, switching between local measurement settings in experiments incurs significant overhead, as reconfiguring optical elements, laser polarizations, or microwave pulses often takes microseconds to milliseconds [31–35]. Moreover, frequent switching can increase control noise, crosstalk, and decoherence. Therefore, optimizing the measurement order of these local measurement settings is crucial.

In this work, we investigate optimal qudit overlapping tomography, in which local measurement settings are constructed from generalized Gell-Mann (GGM) matrices. Motivated by the correspondence between optimal qubit tomography and covering arrays [19], we employ covering arrays to present two explicit constructions of optimal qudit overlapping tomography schemes. For  $n$ -qutrit systems, we prove that pairwise tomography requires at most  $8 + 56 \lceil \log_8 n \rceil$  GGM measurement settings, and we provide an explicit scheme that achieves this bound. Furthermore, we present an efficient algorithm to determine the optimal measurement order. Compared to the worst-case measurement order, our optimal measurement scheme can reduce switching costs by approximately 50%.

The rest of this paper is organized as follows. In Sec. II, we introduce optimal qudit overlapping tomography, covering arrays, and the relationship between them. Sec. III presents two explicit constructions of optimal qudit overlapping tomography. In Sec. IV, we show several upper bounds for optimal qudit overlapping tomography. Sec. V investigates the optimal measurement order. Finally, conclusions are provided in Sec. VI.

\* [shif26@mail.sysu.edu.cn](mailto:shif26@mail.sysu.edu.cn)

## II. OPTIMAL QUDIT OVERLAPPING TOMOGRAPHY AND COVERING ARRAY

In this section, we discuss optimal qudit overlapping tomography, covering arrays, and the relationship between them. For qudit tomography, local measurements are typically performed using the GGM matrices [36], which is defined as follows [37, 38]:

(i)  $\frac{d(d-1)}{2}$  symmetric GGM matrices:

$$\Lambda_s^{jk} = |j\rangle\langle k| + |k\rangle\langle j|, \quad 1 \leq j < k \leq d;$$

(ii)  $\frac{d(d-1)}{2}$  antisymmetric GGM matrices:

$$\Lambda_a^{jk} = -i|j\rangle\langle k| + i|k\rangle\langle j|, \quad 1 \leq j < k \leq d;$$

(iii)  $(d-1)$  diagonal GGM matrices:

$$\Lambda^l = \sqrt{\frac{2}{l(l+1)}} \left( \sum_{j=1}^l |j\rangle\langle j| - |l+1\rangle\langle l+1| \right), \quad 1 \leq l \leq d-1.$$

When  $d = 2$ , the GGM matrices correspond to the Pauli matrices. For simplicity, we denote the  $d^2 - 1$  GGM matrices as  $\{\lambda_i\}_{i=1}^{d^2-1}$  and use  $\lambda_0$  to represent the identity matrix of order  $d$ . Then a  $d$ -dimensional state  $\varrho$  can be written as:

$$\varrho = \sum_{i \in \mathbb{Z}_{d^2}} a_i \lambda_i, \quad (1)$$

where  $a_0 = \frac{1}{d}$ , and  $a_i = \frac{1}{2} \text{Tr}(\lambda_i \varrho)$ . Similarly, an  $n$ -qudit state  $\varrho$  can be written as

$$\varrho = \sum_{(i_1, i_2, \dots, i_n) \in \mathbb{Z}_{d^2}^n} a_{i_1, i_2, \dots, i_n} \lambda_{i_1} \lambda_{i_2} \cdots \lambda_{i_n}, \quad (2)$$

where the tensor product symbols between the matrices  $\lambda_{i_k}$  ( $k = 1, 2, \dots, n$ ) are omitted, and  $a_{i_1, i_2, \dots, i_n} = \frac{1}{d^{n-t} 2^t} \text{Tr}(\lambda_{i_1} \lambda_{i_2} \cdots \lambda_{i_n} \varrho)$  if there are  $t$  nonzero elements in  $(i_1, i_2, \dots, i_n)$ . Thus a full tomography of the  $n$ -qudit state  $\varrho$  can be performed with  $(d^2 - 1)^n$  GGM measurement settings  $\{\lambda_{i_1} \lambda_{i_2} \cdots \lambda_{i_n} \mid i_1 i_2 \cdots i_n \neq 0, (i_1, i_2, \dots, i_n) \in \mathbb{Z}_{d^2}^n\}$ .

The goal of qudit overlapping tomography is to reconstruct all  $k$ -body marginals of an arbitrary  $n$ -qudit state. Obviously, conventional quantum state tomography would require  $(d^2 - 1)^k \binom{n}{k}$  distinct GGM measurement settings [32, 36, 39]. However, this method involves substantial redundancy, since many measurement settings are effectively repeated across different  $k$ -body subsystems. Thus it is important to construct optimal measurement schemes. Next, we introduce optimal qudit overlapping tomography.

**Definition 1** *Optimal qudit overlapping tomography is the problem of determining the minimum number of GGM measurement settings, denoted by  $\phi_k(n, d)$ , required to cover all  $k$ -body marginals of an  $n$ -qudit state.*

For example, in the case of four-qubit state, only nine Pauli measurement settings, namely XXXX, ZYYX, YZZX, YYXY, XZYY, ZXZY, ZZXZ, YXYZ, and XYZZ, are sufficient to reconstruct all 2-body marginals, i.e.,  $\phi_2(4, 2) = 9$  [19]. This is because, for every pair of qubits, these nine combinations of Pauli operators collectively provide the necessary information for state reconstruction. By applying the bijection:  $X \rightarrow 0, Y \rightarrow 1, Z \rightarrow 2$ , the nine Pauli measurement settings can be represented as a  $9 \times 4$  array,

$$\begin{array}{cccc} 0 & 0 & 0 & 0 \\ 2 & 1 & 1 & 0 \\ 1 & 2 & 2 & 0 \\ 1 & 1 & 0 & 1 \\ 0 & 2 & 1 & 1 \\ 2 & 0 & 2 & 1 \\ 2 & 2 & 0 & 2 \\ 1 & 0 & 1 & 2 \\ 0 & 1 & 2 & 2 \end{array} \quad (3)$$

which has the property that in every  $9 \times 2$  subarray, each possible 2-tuple from  $\mathbb{Z}_3 \times \mathbb{Z}_3$  appears exactly once. This property gives rise to a combinatorial object known as a covering array [18].

**Definition 2** *A covering array  $\text{CA}(r; k, n, v)$  is an  $r \times n$  array with entries from an alphabet of size  $v$ , such that in every  $r \times k$  subarray, each possible  $k$ -tuple from  $v \times v \times \cdots \times v$  appears at least once. Given  $k, n$ , and  $v$ , the covering number  $\text{CAN}(k, n, v)$  is the minimum number of rows  $r$  for which a  $\text{CA}(r; k, n, v)$  exists.*

The optimal qubit overlapping tomography using Pauli measurements corresponds to the covering number of covering arrays [19]. Similarly, the optimal qudit overlapping tomography using GGM measurement settings also corresponds to the covering number of covering arrays.

**Observation 1** *The minimum number of GGM measurement settings required to reconstruct all  $k$ -body marginals of an  $n$ -qudit state is equal to the minimum number of rows  $r$  for which a covering array  $\text{CA}(r; k, n, d^2 - 1)$  exists, i.e.,*

$$\phi_k(n, d) = \text{CAN}(k, n, d^2 - 1). \quad (4)$$

Obviously,  $\phi_k(n, d) = \text{CAN}(k, n, d^2 - 1) \geq (d^2 - 1)^k$ . Some tables of covering numbers can be found in Refs. [18, 40]. However, only a small number of covering numbers have been determined explicitly, as the problem of finding the general covering number is NP-hard. In the next section, we present several representative constructions.

### III. CONSTRUCTIONS OF OPTIMAL QUDIT OVERLAPPING TOMOGRAPHY

In this section, we present two explicit constructions of optimal qudit overlapping tomography based on covering arrays. The first construction is based on Zero-Sum construction [18].

**Theorem 1**  $\phi_k(k+1, d) = (d^2 - 1)^k$ .

The construction of a covering array  $\text{CA}((d^2 - 1)^k; k, k+1, d^2 - 1)$  is as follows. List all possible  $k$ -tuples over  $\mathbb{Z}_{d^2-1}$ . For each  $k$ -tuple  $(a_1, a_2, \dots, a_k)$ , define the  $(k+1)$ -th element as  $-(a_1 + a_2 + \dots + a_k)$  (computed modulo  $d^2 - 1$ ). In this way, we obtain a covering array  $\text{CA}((d^2 - 1)^k; k, k+1, d^2 - 1)$  consisting of the rows:

$$(a_1, a_2, \dots, a_k, -(a_1 + a_2 + \dots + a_k)). \quad (5)$$

For example, when  $d = 2$ ,  $k = 2$ , we obtain a covering array  $\text{CA}(9; 2, 3, 3)$  by the above construction:

$$\begin{array}{cccc} 0 & 0 & 0 & 0 \\ 0 & 1 & 2 & \\ 0 & 2 & 1 & \\ 1 & 0 & 2 & \\ 1 & 1 & 1 & \\ 1 & 2 & 0 & \\ 2 & 0 & 1 & \\ 2 & 1 & 0 & \\ 2 & 2 & 2 & \end{array} \quad (6)$$

The second construction is based on Bush's construction [23].

**Theorem 2** When  $d^2 - 1 > k$ , and  $d^2 - 1$  is a prime power, then  $\phi_k(d^2, d) = (d^2 - 1)^k$ .

Note that when  $d^2 - 1$  is a prime power, the possible values for  $d$  are only 2 or 3. Therefore, Theorem 2 holds only for 2 or 3. Here, we need to use Galois field [41]. A Galois field is a field consisting of a finite set of elements, in which addition, subtraction, multiplication, and division (except by zero) are defined and satisfy the field axioms. We usually denote  $\text{GF}(s)$  as the Galois field with  $s$  elements, where  $s$  must be a prime power.

The construction of a covering array  $\text{CA}((d^2 - 1)^k; k, d^2, d^2 - 1)$  is as follows. Consider all polynomials over the finite field  $\text{GF}(d^2 - 1)$  of degree at most  $k-1$ , that is,  $a_0 + a_1 x + a_2 x^2 + \dots + a_{k-1} x^{k-1}$ , where  $a_i \in \text{GF}(d^2 - 1)$  for  $0 \leq i \leq k-1$ . There are exactly  $(d^2 - 1)^k$  such polynomials, which we denote by  $\{f_1, f_2, \dots, f_{(d^2-1)^k}\}$ . Then the covering array  $\text{CA}((d^2 - 1)^k; k, d^2, d^2 - 1)$  is constructed as follows:

$$\begin{array}{ccccc} f_1(\alpha_1) & f_1(\alpha_2) & \cdots & f_1(\alpha_{d^2-1}) & r_1 \\ f_2(\alpha_1) & f_2(\alpha_2) & \cdots & f_2(\alpha_{d^2-1}) & r_2 \\ \vdots & \vdots & \vdots & \vdots & \vdots \\ f_{(d^2-1)^k}(\alpha_1) & f_{(d^2-1)^k}(\alpha_2) & \cdots & f_{(d^2-1)^k}(\alpha_{d^2-1}) & r_{(d^2-1)^k} \end{array}, \quad (7)$$

where  $\alpha_1, \alpha_2, \dots, \alpha_{d^2-1}$  are the  $d^2 - 1$  elements of  $\text{GF}(d^2 - 1)$ , and  $r_i$  is the coefficient of the term  $x^{k-1}$  in the polynomial  $f_i$  for  $1 \leq i \leq (d^2 - 1)^k$ .

Next, we show a simple example. Let  $d = 2$  and  $k = 3$ , then the Galois field  $\text{GF}(3) = \{0, 1, 2\}$ . The 9 polynomials are  $f_1 = 0$ ,  $f_2 = 1$ ,  $f_3 = 2$ ,  $f_4 = x$ ,  $f_5 = 1 + x$ ,  $f_6 = 2 + x$ ,  $f_7 = 2x$ ,  $f_8 = 1 + 2x$ , and  $f_9 = 2 + 2x$ . Then we obtain the covering array  $\text{CA}(9; 2, 4, 3)$ :

$$\begin{array}{cccc} 0 & 0 & 0 & 0 \\ 1 & 1 & 1 & 0 \\ 2 & 2 & 2 & 0 \\ 0 & 1 & 2 & 1 \\ 1 & 2 & 0 & 1 \\ 2 & 0 & 1 & 1 \\ 0 & 2 & 1 & 2 \\ 1 & 0 & 2 & 2 \\ 2 & 1 & 0 & 2 \end{array} \quad (8)$$

When we perform row and column permutations on this array, we would obtain Eq. (3).

### IV. UPPER BOUNDS ON OPTIMAL QUDIT OVERLAPPING TOMOGRAPHY

In this section, we show some upper bounds on optimal qudit overlapping tomography. For small  $d$ ,  $k$ , and  $n$ , we obtain the best known upper bound on  $\phi_k(n, d)$  from the handbook [18] and the website [40], and see Table I.

For general values of  $k$ ,  $n$ , and  $d$ , there is no universal construction for the covering array  $\text{CA}(r; k, n, d^2 - 1)$  when  $r$  is set to the best known upper bound for  $\phi_k(n, d)$ . However, some upper bounds for  $\phi_k(n, d)$  have been established using probabilistic methods.

(1) When  $n \geq k \geq 2$  and  $d \geq 2$ , the following efficient upper bound holds: [42]:

$$\phi_k(n, d) \leq \frac{1}{\log \left( \frac{(d^2-1)^k}{(d^2-1)^k - 1} \right)} \times \left[ \log \binom{n}{k} + k \log(d^2 - 1) + \log \log \left( \frac{(d^2-1)^k}{(d^2-1)^k - 1} \right) + 1 \right]. \quad (9)$$

(2) When  $n \rightarrow \infty$ ,  $n \geq k \geq 2$ , and  $d \geq 2$ , the following upper bound, known as the Stein-Lovász-Johnson (SLJ) bound holds [43–45]:

$$\phi_k(n, d) \leq \frac{k}{\log \frac{(d^2-1)^k}{(d^2-1)^k - 1}} \log n (1 + o(1)). \quad (10)$$

Pairwise tomography ( $k = 2$ ) is the most common form of overlapping tomography. Ref. [46] provides an efficient upper bound for pairwise qubit tomography,  $\phi_2(n, 2) \leq 3 + 6 \lceil \log_3 n \rceil$ , along with an explicit construction. Next, we generalize this result to the qutrit system.

TABLE I. The best known upper bounds on  $\phi_k(n, 2)$  for  $2 \leq k \leq 6$  and  $4 \leq n \leq 20$ , and on  $\phi_k(n, 3)$  for  $2 \leq k \leq 6$  and  $8 \leq n \leq 20$ .

$n$	$\phi_2(n, 2)$	$\phi_3(n, 2)$	$\phi_4(n, 2)$	$\phi_5(n, 2)$	$\phi_6(n, 2)$
4	9	27	81	—	—
5	11	33	81	243	—
6	12	33	111	243	729
7	12	39	123	351	729
8	13	42	135	405	1134
9	13	45	135	405	1377
10	14	45	159	405	1431
11	15	45	159	483	1431
12	15	45	189	483	1455
13	15	45	212	687	2181
14	15	45	231	805	2701
15	15	51	231	842	2901
16	15	51	237	920	3126
17	15	58	237	963	3633
18	15	59	271	1034	3839
19	15	59	271	1064	3961
20	15	59	271	1108	4006
$n$	$\phi_2(n, 3)$	$\phi_3(n, 3)$	$\phi_4(n, 3)$	$\phi_5(n, 3)$	$\phi_6(n, 3)$
8	64	512	4096	32768	262144
9	64	512	4096	32768	262144
10	76	512	6125	53681	450372
11	78	960	7680	61440	450372
12	84	960	7680	61440	491520
13	84	960	7680	61440	520192
14	96	960	7680	65024	753656
15	96	960	7680	65024	753656
16	102	960	8128	94200	753656
17	104	960	8128	94200	753656
18	104	960	8128	94200	782328
19	107	1016	8128	94200	983032
20	108	1016	8184	94200	983032

**Theorem 3** *In an  $n$ -qutrit system,*

$$\phi_2(n, 3) \leq 8 + 56 \lceil \log_8 n \rceil. \quad (11)$$

Theorem 3 shows that, for  $n$ -qutrit overlapping tomography, the number of GGM measurement settings grows only logarithmically with respect to  $n$ . To explicitly construct these GGM measurement settings, it suffices to construct a covering array  $\text{CA}(8 + 56 \lceil \log_8 n \rceil; 2, n, 8)$ . Note that, we use  $\mathbf{i}_n$  to denote a row vector of length  $n$ , in which every element is  $i$ . There are three steps:

1. We need to use  $\text{CA}(64; 2, 8, 8)$  (see Table III in Appendix A) which contains rows  $\{r_i = \mathbf{i}_8\}_{i=0}^7$ , and the remaining rows are denoted by  $\{r_i\}_{i=8}^{63}$ .

2. Next, we need to represent  $0, 1, 2, \dots, n-1$  in base-8 notation. Each element can be written as a column vector of length  $\lceil \log_8 n \rceil$ . In this way, we obtain an array  $A$  of size  $\lceil \log_8 n \rceil \times n$ . For example, when  $n = 10$ , we obtain a  $2 \times 10$  array:

$$A = \begin{matrix} 0 & 0 & 0 & 0 & 0 & 0 & 0 & 0 & 1 & 1 \\ 0 & 1 & 2 & 3 & 4 & 5 & 6 & 7 & 0 & 1 \end{matrix}. \quad (12)$$

3. For each  $r_i$  ( $8 \leq i \leq 63$ ), we replace every element in  $A$  as follows:  $j \rightarrow r_{i,j}$ , where  $0 \leq j \leq 7$ , and  $r_{i,j}$  is the element in the  $j$ -th column of  $r_i$ . Then we obtain a new  $\lceil \log_8 n \rceil \times n$  array  $A_{r_i}$ . Now the covering array

$\text{CA}(8 + 56 \lceil \log_8 n \rceil; 2, n, 8)$  can be constructed as follows:

$$\begin{aligned} & \mathbf{0}_n \\ & \mathbf{1}_n \\ & \vdots \\ & \mathbf{7}_n \\ & A_{r_8} \\ & A_{r_9} \\ & \vdots \\ & A_{r_{63}} \end{aligned} \quad (13)$$

According to the above construction, we have the following corollary.

**Corollary 1** *If there exists a covering array  $\text{CA}((d^2 - 1)^2; 2, d^2 - 1, d^2 - 1)$  that contains the rows  $\{\mathbf{i}_{d^2 - 1}\}_{i=0}^{d^2 - 2}$ , then*

$$\phi_2(n, d) \leq (d^2 - 1) + (d^2 - 1)(d^2 - 2) \lceil \log_{d^2 - 1} n \rceil. \quad (14)$$

Note that when  $d = 2$ , there exists a covering array  $\text{CA}(9; 2, 3, 3)$  that contains the rows  $\{\mathbf{i}_3\}_{i=0}^2$  (see Eq. (6)). Therefore,  $\phi_2(n, 2) \leq 3 + 6 \lceil \log_3 n \rceil$  can be obtained in this way [46].

## V. OPTIMAL MEASUREMENT ORDER

In this section, we consider the problem of determining the optimal measurement order, which minimizes the total overhead associated with switching between measurement settings.

When performing a sequence of local measurements in quantum experiments, switching between different measurement settings is not instantaneous and introduces a non-negligible overhead. Adjustments such as rotating optical elements, tuning laser polarization, or reconfiguring microwave pulses typically require timescales ranging from microseconds to milliseconds [31–35]. Furthermore, frequent switching increases the risk of control noise, crosstalk, and decoherence. Therefore, given a set of required Pauli or GGM basis measurement settings, determining the order of execution that minimizes the total switching cost becomes a sequence optimization problem.

The Hamming distance between two vectors is defined as the number of positions at which their corresponding entries differ [47, 48]. Here, we use the Hamming distance to quantify the switching cost between two local measurements.

**Definition 3** *Give two local GGM measurement settings  $M_i = \lambda_{i_1} \lambda_{i_2} \cdots \lambda_{i_n}$  and  $M_j = \lambda_{j_1} \lambda_{j_2} \cdots \lambda_{j_n}$ , the switching cost between two measurement settings is defined as:*

$$d(M_i, M_j) = |\{k | \lambda_{i_k} \neq \lambda_{j_k}, \forall 1 \leq k \leq n\}|. \quad (15)$$

Given a set of GGM measurements settings,  $\{M_i\}_{i=1}^m$ , our goal is to determine the optimal measurement order

TABLE II. Minimum cost and maximum cost for CA (33,3,6,3).

0 1 2 2 1 0	0 1 2 2 1 0 (cost: 3)
0 1 2 0 2 1	(cost: 3)
0 2 2 1 0 1	(cost: 3)
0 0 2 1 1 2	(cost: 3)
0 1 0 1 2 2	(cost: 3)
0 1 1 2 0 2	(cost: 3)
0 0 1 2 2 1	(cost: 3)
1 0 2 2 0 1	(cost: 3)
2 1 0 2 0 1	(cost: 3)
0 2 0 2 1 1	(cost: 3)
0 2 1 0 1 2	(cost: 3)
1 0 1 0 2 2	(cost: 3)
1 0 2 1 2 0	(cost: 3)
1 1 0 2 2 0	(cost: 3)
2 1 1 0 2 0	(cost: 3)
0 2 1 1 2 0	(cost: 3)
2 2 0 1 1 0	(cost: 3)
1 2 0 1 0 2	(cost: 3)
1 0 0 2 1 2	(cost: 3)
1 0 1 1 0 2	(cost: 3)
1 1 1 1 1 1	(cost: 3)
2 2 1 0 0 1	(cost: 4)
1 2 0 0 2 1	(cost: 3)
1 2 2 0 1 0	(cost: 3)
2 0 2 0 1 1	(cost: 3)
2 1 0 0 1 2	(cost: 3)
1 1 2 0 0 2	(cost: 3)
2 1 2 1 0 0	(cost: 3)
0 1 0 1 0 0	(cost: 2)
0 0 0 0 0 0	(cost: 2)
2 0 0 1 2 1	(cost: 4)
2 0 1 2 1 0	(cost: 4)
2 2 2 2 2 2	(cost: 4)
Minimum cost: 98	Maximum cost: 185

that minimizes the total switching cost between these measurements. Specifically, we need to find a permutation  $\pi : [m] \rightarrow [m]$  that minimizes the total cost:

$$\text{Total cost} = \sum_{i=1}^{m-1} d(M_{\pi(i)}, M_{\pi(i+1)}). \quad (16)$$

The optimization problem can be formulated as:

$$\text{Minimum cost} = \min_{\pi \in S_m} \sum_{i=1}^{m-1} d(M_{\pi(i)}, M_{\pi(i+1)}) \quad (17)$$

where  $S_m$  is the set of all permutations of  $m$  elements.

This problem can be essentially transformed into the shortest Hamiltonian path problem on a complete weighted graph  $K_m$ , where each node  $v_i$  corresponds to the  $i$ -th measurement configuration  $M_i$ , and the weight of edge  $e_{ij}$  is  $w_{ij} = d(M_i, M_j)$ .

Various methods have been studied for the shortest Hamiltonian path problem [49–52]. While dynamic programming is often used, considering that the number of qudits and measurement settings might be very large, we propose a hybrid algorithm combining dynamic programming (for small-scale problems), an improved cluster-based nearest neighbor + 2-opt heuristic algorithm (for medium-scale problems), and simulated annealing (for

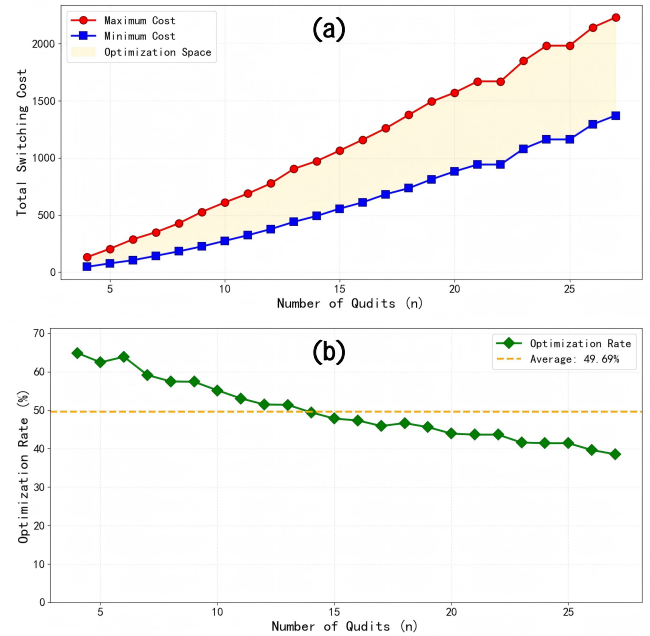


FIG. 1. Comparison between the optimal measurement order and the worst measurement order. (a). The red line represents the minimum cost achieved by the optimal measurement order, while the blue line represents the maximum cost corresponding to the worst measurement order, as the number of qudits increases from 4 to 27. The yellow region indicates the portion of cost that is reduced through optimization. (b) The green line represents the optimization rate, which is calculated as  $\frac{\text{Maximum cost} - \text{Minimum cost}}{\text{Maximum cost}} \times 100\%$ .

large-scale problems). The specific algorithm or pseudocode is provided in Appendix B. Below, we give an example.

We consider the covering array CA(33; 3, 6, 3), which corresponds to the construction of the optimal qudit overlapping tomography with  $\phi_3(6, 2) = 33$ . Table II shows both the optimal measurement order along with its minimum cost, as well as the worst measurement order with its maximum cost. The algorithm used to determine the maximum cost is similar to the optimization algorithm, but with the objective reversed. By comparing these two tables, we observe that optimization reduces the total cost from 185 to 98, achieving an improvement of nearly 50%.

Since there is currently no program or method capable of constructing all types of small-scale optimal covering arrays, we can instead use the IPOG-F algorithm from [53] to generate near-optimal covering arrays for our experiments. Based on the IPOG-F algorithm, we generated 24 covering arrays with fixed  $d = 2$ ,  $k = 3$ , and  $n$  ranging from 4 to 27. Using these covering arrays, we conducted simulation experiments on a computer and plotted the maximum and minimum costs as functions of  $n$  (ranging from 4 to 27), as shown in Figure 1. Compared to the worst-case ordering, our optimized schedule

reduces switching costs by approximately 50%, as indicated in the figure.

## VI. CONCLUSIONS

In this work, we have investigated optimal qudit overlapping tomography using GGM measurement settings. By employing covering arrays, we presented two constructions for optimal qudit overlapping tomography schemes. For  $n$ -qutrit systems, we established an upper bound of  $8 + 56 \lceil \log_8 n \rceil$  measurement settings for pairwise tomography and provided an explicit scheme that achieves this bound. Furthermore, we introduced an algorithm to optimize the measurement order, reducing experimental switching costs by approximately 50% compared to the worst-case scenario.

Our results bridge a critical gap in quantum state characterization by enabling efficient overlapping tomography for qudit systems, which are increasingly relevant in quantum communication, error correction, and simulation. The reduction in measurement settings and optimized switching order not only to theoretical efficiency but also to practical feasibility in experimental implementations, where measurement reconfiguration overhead and noise are major concerns. Given that optimal pairwise overlapping tomography for six-qubit systems has already been implemented on optical platforms [19], realizing our proposed optimal overlapping qudit tomography scheme on experimental platforms is also of significant importance and research value. Another interesting direction is to study optimal overlapping tomography in mixed systems by using mixed covering arrays.

## ACKNOWLEDGMENTS

We thank Qi Zhao, Xingjian Zhang, Tianfeng Feng, Huan Cao, and Dian Wu for discussing this problem.

---

[1] K. Vogel and H. Risken, *Phys. Rev. A* **40**, 2847 (1989).

[2] A. I. Lvovsky and M. G. Raymer, *Rev. Mod. Phys.* **81**, 299 (2009).

[3] G. M. D'ARIANO, Advances in imaging and electron physics **128**, 205 (2003).

[4] N. Linden, S. Popescu, and W. K. Wootters, *Phys. Rev. Lett.* **89**, 207901 (2002).

[5] A. C. Doherty, P. A. Parrilo, and F. M. Spedalieri, *Phys. Rev. A* **69**, 022308 (2004).

[6] J. R. Garrison and T. Grover, *Phys. Rev. X* **8**, 021026 (2018).

[7] J. Eisert, M. Friesdorf, and C. Gogolin, *Nat. Phys.* **11**, 124–130 (2015).

[8] M. Cramer, M. B. Plenio, S. T. Flammia, R. Somma, D. Gross, S. D. Bartlett, O. Landon-Cardinal, D. Poulin, and Y.-K. Liu, *Nat. Commun.* **1**, 149 (2010).

[9] J. Cotler and F. Wilczek, *Phys. Rev. Lett.* **124**, 100401 (2020).

[10] K. Berrada, S. Abdel-Khalek, E. Khalil, A. Alkaoud, and H. Eleuch, *Chaos Soliton Fract.* **164**, 112621 (2022).

[11] L. T. Weinbrenner, N. Prasannan, K. Hansenne, S. Denker, J. Sperling, B. Brecht, C. Silberhorn, and O. Gühne, *Phys. Rev. Lett.* **132**, 240802 (2024).

[12] Y.-L. Mao, H. Chen, B. Guo, S. Liu, Z.-D. Li, M.-X. Luo, and J. Fan, *Phys. Rev. Lett.* **132**, 240801 (2024).

[13] B. G. M. Araújo, M. M. Taddei, D. Cavalcanti, and A. Acín, *Phys. Rev. A* **106**, 062441 (2022).

[14] J. Wang, S. Paesani, R. Santagati, S. Knauer, A. A. Gentile, N. Wiebe, M. Petruzzella, J. L. O'Brien, J. G. Rarity, A. Laing, and M. G. Thompson, *Nat. Phys.* **13**, 551–555 (2017).

[15] T. J. Evans, R. Harper, and S. T. Flammia, [arXiv: 1912.07636](https://arxiv.org/abs/1912.07636) (2019).

[16] V. Gebhart, R. Santagati, A. A. Gentile, E. M. Gauger, D. Craig, N. Ares, L. Banchi, F. Marquardt, L. Pezzè, and C. Bonato, *Nat. Rev. Phys.* (2023).

[17] H.-Y. Huang, Y. Tong, D. Fang, and Y. Su, *Phys. Rev. Lett.* **130**, 200403 (2023).

[18] C. J. Colbourn, *CRC handbook of combinatorial designs* (CRC press, 2010).

[19] K. Hansenne, R. Qu, L. T. Weinbrenner, C. de Gois, H. Wang, Y. Ming, Z. Yang, P. Horodecki, W. Gao, and O. Gühne, *Phys. Rev. Lett.* **135**, 060801 (2025).

[20] Z. Yang, S. Ru, L. Cao, N. Zheludev, and W. Gao, *Phys. Rev. Lett.* **130**, 050804 (2023).

[21] C. Wei, K. Yang, L. Che, F. Xu, J. Song, and T. Xin, *Phys. Rev. Appl.* **24**, 044091 (2025).

[22] C. J. Colbourn, *Le Matematiche* **59**, 125 (2004).

[23] A. S. Hedayat, N. J. A. Sloane, and J. Stufken, *Orthogonal arrays: theory and applications* (Springer Science & Business Media, 2012).

[24] D. Kuhn, D. Wallace, and A. Gallo, *IEEE Trans. Softw. Eng.* **30**, 418 (2004).

[25] D. R. Kuhn, R. N. Kacker, and Y. Lei, *Introduction to combinatorial testing* (CRC press, 2013).

[26] D. Bruß and C. Macchiavello, *Phys. Rev. Lett.* **88**, 127901 (2002).

[27] N. J. Cerf, M. Bourennane, A. Karlsson, and N. Gisin, *Phys. Rev. Lett.* **88**, 127902 (2002).

[28] H. Bechmann-Pasquinucci and A. Peres, *Phys. Rev. Lett.* **85**, 3313 (2000).

[29] S. Etcheverry, G. Cañas, E. S. Gómez, W. A. T. Nogueira, C. Saavedra, G. B. Xavier, and G. Lima, *Sci. Rep.* **3** (2013).

[30] M. Erhard, M. Krenn, and A. Zeilinger, *Nat. Rev. Phys.* **2**, 365–381 (2020).

[31] P. Six, P. Campagne-Ibarcq, I. Dotsenko, A. Sarlette, B. Huard, and P. Rouchon, *Phys. Rev. A* **93**, 012109 (2016).

[32] J. Li, S. Huang, Z. Luo, K. Li, D. Lu, and B. Zeng, *Phys. Rev. A* **96**, 032307 (2017).

[33] R. Stricker, M. Meth, L. Postler, C. Edmunds, C. Ferrie, R. Blatt, P. Schindler, T. Monz, R. Kueng, and M. Ringbauer, *PRX Quantum* **3**, 040310 (2022).

[34] S. E. Smart and D. A. Mazziotti, *Phys. Rev. A* **103**, 012420 (2021).

[35] N. Friis, O. Marty, C. Maier, C. Hempel, M. Holzäpfel, P. Jurcevic, M. B. Plenio, M. Huber, C. Roos, R. Blatt, and B. Lanyon, *Phys. Rev. X* **8**, 021012 (2018).

[36] R. T. Thew, K. Nemoto, A. G. White, and W. J. Munro, *Phys. Rev. A* **66**, 012303 (2002).

[37] G. Kimura, *Phys. Lett. A* **314**, 339–349 (2003).

[38] R. A. Bertlmann and P. Krammer, *J. Phys. A: Math. Theor.* **41**, 235303 (2008).

[39] D. F. V. James, P. G. Kwiat, W. J. Munro, and A. G. White, *Phys. Rev. A* **64**, 052312 (2001).

[40] C. Colbourn, *Catales*.

[41] R. Lidl and H. Niederreiter, *Finite fields*, 20 (Cambridge university press, 1997).

[42] K. Sarkar and C. J. Colbourn, *SIAM J. Discrete Math.* **31**, 1277 (2017).

[43] D. S. Johnson, in *Proceedings of the Fifth Annual ACM Symposium on Theory of Computing*, STOC '73 (Association for Computing Machinery, New York, NY, USA, 1973) p. 38–49.

[44] L. Lovász, *Discrete Math.* **13**, 383 (1975).

[45] S. Stein, *J. Comb. Theory Ser. A* **16**, 391 (1974).

[46] G. García-Pérez, M. A. C. Rossi, B. Sokolov, E.-M. Borrelli, and S. Maniscalco, *Phys. Rev. Res.* **2**, 023393 (2020).

[47] R. W. Hamming, *Bell Syst. Tech. J.* **29**, 147 (1950).

[48] F. J. MacWilliams and N. J. A. Sloane, *The theory of error-correcting codes*, Vol. 16 (Elsevier, 1977).

[49] M. Held and R. M. Karp, *J. Soc. Ind. Appl. Math.* **10**, 196 (1962).

[50] E. Cela, V. G. Deineko, and G. J. Woeginger, *Discrete Appl. Math.* **354**, 3–14 (2024).

[51] H.-C. An, R. Kleinberg, and D. B. Shmoys, *J. ACM* **62** (2015).

[52] A. Madkour, W. G. Aref, F. U. Rehman, M. A. Rahman, and S. Basalamah, [arXiv: 1705.02044](https://arxiv.org/abs/1705.02044) (2017).

[53] M. Forbes, J. Lawrence, Y. Lei, R. N. Kacker, and D. R. Kuhn, *J. Res. Nat. Inst. Stand. Technol.* **113**, 287 (2008).

**Appendix A: CA(64; 2, 8, 8)**

TABLE III. CA(64; 2, 8, 8)

$r_0=0$	0 0 0 0 0 0 0 0	$r_{16}=1$	4 7 2 6 5 3 0	$r_{32}=3$	6 2 4 1 7 5 0	$r_{48}=5$	1 4 6 3 2 7 0
$r_1=1$	1 1 1 1 1 1 1 1	$r_{17}=1$	7 2 6 5 3 0 4	$r_{33}=3$	2 4 1 7 5 0 6	$r_{49}=5$	4 6 3 2 7 0 1
$r_2=2$	2 2 2 2 2 2 2 2	$r_{18}=1$	2 6 5 3 0 4 7	$r_{34}=3$	4 1 7 5 0 6 2	$r_{50}=6$	5 7 4 3 1 0 2
$r_3=3$	3 3 3 3 3 3 3 3	$r_{19}=1$	6 5 3 0 4 7 2	$r_{35}=3$	1 7 5 0 6 2 4	$r_{51}=6$	7 4 3 1 0 2 5
$r_4=4$	4 4 4 4 4 4 4 4	$r_{20}=1$	5 3 0 4 7 2 6	$r_{36}=4$	2 1 6 0 7 3 5	$r_{52}=6$	4 3 1 0 2 5 7
$r_5=5$	5 5 5 5 5 5 5 5	$r_{21}=1$	3 0 4 7 2 6 5	$r_{37}=4$	1 6 0 7 3 5 2	$r_{53}=6$	3 1 0 2 5 7 4
$r_6=6$	6 6 6 6 6 6 6 6	$r_{22}=2$	4 0 5 1 3 7 6	$r_{38}=4$	6 0 7 3 5 2 1	$r_{54}=6$	1 0 2 5 7 4 3
$r_7=7$	7 7 7 7 7 7 7 7	$r_{23}=2$	0 5 1 3 7 6 4	$r_{39}=4$	0 7 3 5 2 1 6	$r_{55}=6$	0 2 5 7 4 3 1
$r_8=0$	1 2 3 4 5 6 7	$r_{24}=2$	5 1 3 7 6 4 0	$r_{40}=4$	7 3 5 2 1 6 0	$r_{56}=6$	2 5 7 4 3 1 0
$r_9=0$	2 3 4 5 6 7 1	$r_{25}=2$	1 3 7 6 4 0 5	$r_{41}=4$	3 5 2 1 6 0 7	$r_{57}=7$	3 6 1 5 4 2 0
$r_{10}=0$	3 4 5 6 7 1 2	$r_{26}=2$	3 7 6 4 0 5 1	$r_{42}=4$	5 2 1 6 0 7 3	$r_{58}=7$	6 1 5 4 2 0 3
$r_{11}=0$	4 5 6 7 1 2 3	$r_{27}=2$	7 6 4 0 5 1 3	$r_{43}=5$	6 3 2 7 0 1 4	$r_{59}=7$	1 5 4 2 0 3 6
$r_{12}=0$	5 6 7 1 2 3 4	$r_{28}=2$	6 4 0 5 1 3 7	$r_{44}=5$	3 2 7 0 1 4 6	$r_{60}=7$	5 4 2 0 3 6 1
$r_{13}=0$	6 7 1 2 3 4 5	$r_{29}=3$	7 5 0 6 2 4 1	$r_{45}=5$	2 7 0 1 4 6 3	$r_{61}=7$	4 2 0 3 6 1 5
$r_{14}=0$	7 1 2 3 4 5 6	$r_{30}=3$	5 0 6 2 4 1 7	$r_{46}=5$	7 0 1 4 6 3 2	$r_{62}=7$	2 0 3 6 1 5 4
$r_{15}=1$	0 4 7 2 6 5 3	$r_{31}=3$	0 6 2 4 1 7 5	$r_{47}=5$	0 1 4 6 3 2 7	$r_{63}=7$	0 3 6 1 5 4 2

**Appendix B: Optimal measurement order algorithm**

As mentioned in the main text, we consider an adaptive algorithm that integrates dynamic programming, heuristic algorithms, and simulated annealing to optimize the sequence of measurement settings. The algorithm consists of two parts: a main program and the subfunctions required to implement the main program, as shown below.

---

**Algorithm 1:** Qudit Measurement Sequence Optimization - Main Algorithm

---

**Input** : Measurement configurations  $\mathcal{C} = \{c_1, c_2, \dots, c_n\}$ , qudit dimension  $d$ , optimization method  $m$   
**Output:** Optimized sequence  $\pi^*$  with minimum switching cost, total cost  $C_{\text{total}}$

```

// Phase 1: Cost Matrix Construction with Caching
 $C \leftarrow$  zero matrix of size  $n \times n$ ;
 $\mathcal{P} \leftarrow \emptyset$ ; // Set of parsed configurations
for  $i = 1$  to  $n$  do
   $p_i \leftarrow \text{ParseMeasurementConfig}(c_i)$  ; // Parse into tuple for hashing
   $\mathcal{P} \leftarrow \mathcal{P} \cup \{p_i\}$ ;
for  $i = 1$  to  $n$  do
  for  $j = i + 1$  to  $n$  do
     $d_{ij} \leftarrow \text{ComputeHammingDistance}(p_i, p_j)$  ; // Cached Hamming distance
     $C[i, j] \leftarrow d_{ij}$ ,  $C[j, i] \leftarrow d_{ij}$  ; // Symmetric matrix

// Phase 2: Adaptive Algorithm Selection
switch  $m$  do
  case 'exact' do
    // Held-Karp with memory optimization
    Initialize  $dp$  as dictionary,  $parent$  as dictionary;
    for  $i = 1$  to  $n$  do
       $dp[\{i\}, i] \leftarrow 0$  ; // Single-node paths
    for  $k = 2$  to  $n$  do
      for each subset  $S$  with  $|S| = k$  do
        for each  $j \in S$  do
           $prev \leftarrow S \setminus \{j\}$ ;
           $dp[S, j] \leftarrow \min_{i \in prev} \{dp[prev, i] + C[i, j]\}$ ;
          Store  $parent[S, j] \leftarrow \arg \min_{i \in prev} \{dp[prev, i] + C[i, j]\}$ ;
     $\pi^* \leftarrow \text{backtrack from } \min_j dp[\{1, \dots, n\}, j]$ ;
  case 'heuristic' do
    // Enhanced clustering + 2-opt
     $\pi_{\text{init}} \leftarrow \text{ClusterNearestNeighborV2}(C, \mathcal{P})$  ; // Improved clustering NN
     $\pi^* \leftarrow \text{TwoOptOptimizationV2}(\pi_{\text{init}}, C)$  ; // Time-limited 2-opt
  case 'sa' do
     $\pi_{\text{init}} \leftarrow \text{ClusterNearestNeighborV2}(C, \mathcal{P})$  ; // Good initial solution
     $\pi^* \leftarrow \text{SimulatedAnnealing}(C, \pi_{\text{init}})$  ; // Simulated annealing
  case 'auto' do
    if  $n \leq 12$  then
      Use exact method;
    else
      if  $n \leq 50$  then
        Use heuristic method;
      else
        Use simulated annealing;

// Phase 3: Performance Evaluation
 $C_{\text{total}} \leftarrow \sum_{i=1}^{n-1} C[\pi_i^*, \pi_{i+1}^*]$ ;
 $C_{\text{random}} \leftarrow$  average cost of random permutations;
improvement  $\leftarrow \frac{C_{\text{random}} - C_{\text{total}}}{C_{\text{random}}} \times 100\%$ ;
return  $\pi^*$ ,  $C_{\text{total}}$ , improvement

```

---

---

**Algorithm 2:** Cluster-based Nearest Neighbor Algorithm

---

```

Function ClusterNearestNeighborV2( $C, \mathcal{P}$ ):
  // Feature-based clustering using basis type statistics
  for  $i = 1$  to  $n$  do
     $\mathbf{f}_i \leftarrow [\text{count}_a(p_i), \text{count}_b(p_i), \text{count}_c(p_i)]$ ; // Basis type features
     $\{\mathcal{K}_1, \dots, \mathcal{K}_k\} \leftarrow \text{K-means clustering of } \{\mathbf{f}_1, \dots, \mathbf{f}_n\};$ 
    // Greedy cluster ordering by connectivity
     $\text{order} \leftarrow [\arg \max_j |\mathcal{K}_j|];$  // Start with largest cluster
     $\text{remaining} \leftarrow \{1, \dots, k\} \setminus \text{order};$ 
    while  $\text{remaining} \neq \emptyset$  do
       $c_{\text{current}} \leftarrow \text{all nodes in clusters currently in order};$ 
       $j^* \leftarrow \arg \min_{j \in \text{remaining}} \min_{u \in c_{\text{current}}, v \in \mathcal{K}_j} C[u, v];$ 
      Append  $j^*$  to  $\text{order}$ , remove from  $\text{remaining}$ ;
    // Nearest neighbor within each cluster
     $\pi \leftarrow \emptyset;$ 
    for  $j \in \text{order}$  do
      if  $\pi = \emptyset$  then
         $v \leftarrow \text{first node in } \mathcal{K}_j;$ 
      else
         $v \leftarrow \arg \min_{u \in \mathcal{K}_j} C[\pi_{\text{last}}, u];$ 
       $\text{visited} \leftarrow \{v\}$ , append  $v$  to  $\pi$ ;
      while  $\text{visited} \neq \mathcal{K}_j$  do
         $v \leftarrow \arg \min_{u \in \mathcal{K}_j \setminus \text{visited}} C[v, u];$ 
        Append  $v$  to  $\pi$ , add  $v$  to  $\text{visited}$ ;
    return  $\pi$ 

```

---



---

**Algorithm 3:** 2-Opt Local Optimization Algorithm

---

```

Function TwoOptOptimizationV2( $\pi, C$ ):
   $\pi_{\text{current}} \leftarrow \pi$ ,  $\text{improved} \leftarrow \text{true};$ 
   $\text{startTime} \leftarrow \text{currentTime}();$ 
  while  $\text{improved}$  and  $(\text{currentTime}() - \text{startTime}) < t_{\max}$  do
     $\text{improved} \leftarrow \text{false};$ 
    for  $i = 1$  to  $|\pi| - 2$  do
      for  $j = i + 2$  to  $|\pi|$  do
        // Incremental cost calculation
        if  $j + 1 \leq |\pi|$  then
           $\Delta \leftarrow (C[\pi_i, \pi_j] + C[\pi_{i+1}, \pi_{j+1}]) - (C[\pi_i, \pi_{i+1}] + C[\pi_j, \pi_{j+1}]);$ 
        else
           $\Delta \leftarrow C[\pi_i, \pi_j] - C[\pi_i, \pi_{i+1}];$ 
        if  $\Delta < 0$  then
          Reverse segment  $\pi[i + 1 : j]$  in  $\pi_{\text{current}};$ 
           $\text{improved} \leftarrow \text{true};$ 
          break;
        if  $\text{improved}$  then
          break
    return  $\pi_{\text{current}}$ 

```

---

---

**Algorithm 4:** Simulated Annealing Algorithm

---

```

Function SimulatedAnnealing( $C, \pi_{init}$ ):
   $T \leftarrow T_0, \pi_{current} \leftarrow \pi_{init};$ 
   $\pi_{best} \leftarrow \pi_{init}, E_{best} \leftarrow \text{cost}(\pi_{init});$ 
  for  $iter = 1$  to  $iter_{max}$  do
    // Generate neighbor solution
    if  $\text{random}() < 0.5$  then
      // 2-opt move
       $i, j \leftarrow$  random indices with  $i < j - 1$ ;
       $\pi' \leftarrow \pi_{current}[1 : i] + \text{reverse}(\pi_{current}[i + 1 : j]) + \pi_{current}[j + 1 :];$ 
    else
      // Swap move
       $\pi' \leftarrow \pi_{current};$ 
       $i, j \leftarrow$  two distinct random indices;
      Swap  $\pi'[i]$  and  $\pi'[j]$ ;
    // Metropolis acceptance criterion
     $\Delta E \leftarrow \text{cost}(\pi') - \text{cost}(\pi_{current});$ 
    if  $\Delta E < 0$  or  $\text{random}() < \exp(-\Delta E/T)$  then
       $\pi_{current} \leftarrow \pi';$ 
    // Update best solution
    if  $\text{cost}(\pi_{current}) < E_{best}$  then
       $\pi_{best} \leftarrow \pi_{current};$ 
       $E_{best} \leftarrow \text{cost}(\pi_{current});$ 
     $T \leftarrow \alpha \cdot T;$  // Geometric cooling
    if  $T < T_{min}$  then
      break
  return  $\pi_{best}$ 

```

---